Title

Technical note: Low-cost MR-compatible pneumatic respiratory organ motion simulator for the development of MR-guided thermal therapy

Journal

Medical Physics, 49(7)

ISSN

0094-2405

Authors

Kim, Kisoo
Jones, Peter
Diederich, Chris
et al.

Publication Date

2022-07-01

DOI

10.1002/mp.15783

Title:

Technical Note: Low-cost MR-compatible pneumatic respiratory organ motion simulator for development of MR-guided thermal therapy

Authors: Kisoo Kim[1*], Peter Jones[2], Chris Diederich[2], Eugene Ozhinsky[1]
1. Department of Radiology & Biomedical Imaging, University of California, San Francisco, USA
2. Department of Radiation Oncology, University of California, San Francisco, USA

Subheadings: Low-cost respiratory motion simulator

*Correspondence:
Kisoo Kim, Ph.D.
Department of Radiology & Biomedical Imaging
University of California, San Francisco
2340 Sutter Street, S341,
94115 San Francisco, California, USA
415-260-5978
ki-soo.kim@ucsf.edu

Abstract

Background: In MR-guided thermal therapy, respiratory motion can cause a significant temperature error in MR thermometry and reduce the efficiency of the treatment. A respiratory motion simulator is necessary for development of new MR imaging and motion compensation techniques.

Purpose: The purpose of this study is to develop a low-cost and simple MR-compatible respiratory motion simulator to support proof-of-concept studies of MR monitoring approaches with respiratory-induced abdominal organ motion.

Methods: The phantom motion system integrates pneumatic control via an actuator subsystem located outside the MRI and coupled via plastic tubing to a compressible bag for distention and retraction within the MRI safe motion subsystem and phantom positioned within the MRI scanner. Performance of the respiratory motion simulator was evaluated with a real-time gradient echo MRI pulse sequence.

Results: The motion simulator can produce respiratory rates in the range of 8-16 breaths/min. Our experiments showed the consistent periodic motion of the phantom during MRI acquisition in the range of 3.7 – 9 mm with 16 breaths/min. The operation of the simulator did not cause interference with MRI acquisition.

Conclusions: In this study, we have demonstrated the ability of the motion simulator to generate controlled respiratory motion of a phantom. The low-cost MR-compatible respiratory motion simulator can be easily constructed from off-the-shelf and 3D-printed parts based on open-source 3D models and instructions. This could lower the barriers to the development of new MR imaging techniques with motion compensation.

Keywords: respiratory motion, abdomen, MR-compatible, MRgFUS, motion simulator

1. Introduction

Abdominal organ motion causes significant errors in magnetic resonance (MR) imaging when applied to MR-guided therapies of abdominal or pelvic organs due to organ shift and deformation.[1,2] MR-guided focused ultrasound (MRgFUS) therapy performs non-invasive heat delivery under MR supervision that can provide for accurate targeting and non-invasive temperature measurement for therapy control and verification. Clinical MRgFUS systems are currently used for the ablation of deep soft tissue tumors in sites such as the brain, uterine fibroids, prostate, pancreas, and bone metastases.[3,4] Recent innovations are expanding the use of these MRgFUS systems for the delivery of long-duration hyperthermia over larger and deep volumes.[5,6] MR thermometry allows for real-time temperature measurement over treatment volumes to ensure patient safety and precise heat deposition during the ablation procedure.

Proton resonance frequency shift (PRFS) is the most common and accurate method of MR temperature monitoring. However, this approach is susceptible to motion artifacts. Thus, abdominal organ motion causes significant errors in MR thermometry of abdominal and pelvic organs.[7,8] In addition, the efficiency of localizing ultrasound energy to the target is reduced due to the target zone moving away from the focus position, necessitating gating or more diffuse treatment zones.[2] Since respiration is the main source of abdominal organ motion, compensation techniques for respiratory motion have been proposed and developed to reduce temperature

errors in MR thermometry. Most of these studies have designed and used a custom-made respiratory motion phantom to validate their technology.[9–12]

Respiration motion-robust 4D MRI techniques have been developed to assess patient-specific breathing motion for radiation treatment planning and delivery.[1,13,14] A commercial dynamic motion phantom has been used for the end-to-end verification of MRI-LINAC radiation therapy system.[15,16] It is not a practical option for most acquisition technique development studies due to its high cost.

There is a need for dynamic motion phantoms in the early stages of the development of new, motion-robust, and fast MR imaging techniques in abdominal organs. Several custom-made respiratory phantoms have been developed to evaluate motion compensation in MR imaging techniques. [9,13,17,18] For instance, Maier-Hein et al. developed a respiratory liver motion simulator for validating image-guided tumor biopsy procedures.[17] The simulator provided a human torso model, and an artificial diaphragm was mounted and simulated the liver movement by using a lung ventilator.

For new studies, the design and fabrication of a motion simulator from scratch may create a significant obstacle and increase the complexity of the project. Descriptions of motion simulator designs found in literature often lack the details, necessary to easily reproduce them. The goal of this study was to develop a low-cost, easy-to-make respiratory motion simulator to simulate respiration-induced abdominal organ motion inside the MRI bore.

2. Materials and Methods

2.A Respiratory motion simulator

The respiratory motion simulator was designed based on the fabrication methods and components used in earlier approaches.[9,13,17,18] Our design improves on them by offering a low-cost and simple fabrication process.

As shown in Fig.1, the respiratory motion simulator consists of two main parts: 1) Motion actuator placed outside the MRI scanner; 2) Motion phantom placed inside the MRI scanner. The linear actuator moves in a linear motion that can increase or decrease the pressure inside the bag valve mask (BVM, volume: 1.8 L). The BVM is coupled via a flexible polymer tubing (Tygon) to the compressible bag in the motion phantom in the MRI scanner (Fig 1b). Finally, cyclical motion can be pneumatically applied to the MRI by the motion actuator.

The motion actuator consisted of a DC motor, a motor controller, a 3D-printed linear actuator, and the BVM. The DC motor featured a torque of 6.8649 N·m and could be operated at a speed of 8-16 revolutions per minute. The motor controller allowed adjusting the speed of the DC motor in the range of 8-16 cycles per minute. The linear actuator was connected to the DC motor to convert the motor rotation into linear motion. The linear actuator was 3D printed with Acrylonitrile Butadiene Styrene (ABS) materials. The motion of the actuator controlled the level of inflation or deflation of the BVM.

The motion phantom was constructed from non-metallic 3D-printed parts and rubber bands. As shown in Fig.2, an inflatable bag (reservoir bag for the BVM) was placed inside the motion phantom to simulate the lung motion. A 10 × 10 cm^2 square plate (Fig.2a, b) generated motion to simulate the shift of abdominal organs by the diaphragm.

Elastic rubber bands in the motion phantom assembly provided the passive compression force necessary to cyclically pull the tissue-mimicking phantom back to the original position and re-inflating the BVM when not under compression. Since the inflatable bag in the motion phantom

was coupled with the BVM, the rotary motion of the motor produced periodic motion of the phantom. The custom phantom holder featured non-metallic wheels and a circular opening to allow the propagation of ultrasound beam for experiments with MRgFUS transducers. The holder was attached to the square plate in the motion phantom. Finally, a tissue-mimicking focused ultrasound phantom (weight=1.2 kg, InSightec, Haifa, Israel) was placed on top of the plastic holder.

In the motion actuator, the volume of BVM was controlled by adding a plastic plate into a space between the BVM and the linear actuator (Fig.2e, f). When a piston of the linear actuator pressed the BVM, the reduced volume of BVM increased the level of compression, resulting in an increase in the displacement. The choice of plastic plate resulted in different amounts of displacement. All custom parts of the motion actuator and phantom could be 3D-printed from the open-source models and assembled by following the instructions, published on GitHub.[19]

2.B Evaluation of Motion Simulator

The motion simulator was evaluated with a tissue-mimicking HIFU phantom in a 3T MRI scanner (GE Healthcare, Waukesha, WI). Figure 3 shows an example of the placement of a motion phantom in the MRI scanner. The motion phantom was connected via the Tygon tube to the motion actuator including the DC motor, which was located outside the MRI scanner. In this study, the respiratory rate of 16 breaths/min was set up. Without ultrasound heating, the consistency of movement was evaluated using a fast MRI scanning sequence integrated with a navigator MR sequence, which allowed the real-time measurement of displacement.

2.B.1 Experimental setup

The accelerated MR imaging application was built on the RTHawk Research Platform (HeartVista, Menlo Park, CA).[20,21] It featured an accelerated GRE sequence with a spiral readout trajectory to achieve real-time MR imaging.

Respiratory motion was tracked with an integrated pencil-beam navigator sequence and quantified with a temporal window of 17 ms. Once an MR image is obtained, a pencil beam navigator measured the displacement of the phantom. MRI parameters included as follows: TR=25 ms, TE=14.8 ms, FOV= 280 ×280 mm, matrix=158, readout interleave=11, and TR of pencil beam navigator = 17 ms. Navigators were set on the center of the phantom in a sagittal plane to track the movement. The phantom was placed on the plastic holder with wheels and was moving along the axis of the MRI bore. Magnitude images on the coronal plane were reconstructed with the navigator tracking sequence. In this study, four different volumes of the BVM were tested using differently sized plastic plates. Real-time displacement was measured for the duration of 3 mins.

2.B.2 Data analysis

For the analysis, recorded measurements of navigator positions were normalized first and used to quantify cyclical motion in each 3-minute experiment. To measure the displacement, a pair of images, corresponding to the maximum and minimum navigator positions (peak-to-peak) in one of the respiratory cycles, was converted to binary images and subtracted from each other (Fig.4). Measured displacement from those images was used to convert normalized navigator positions into the total displacement.

3. Results

Figure 4 shows the time-dependent displacement of the phantom in the MRI scanner, with the 1.65 L volume of the BVM and 16 breaths/min. The MR magnitude images (Fig.4a) represent the maximum and minimum navigator positions in one of the respiratory cycles. The subtracted binary image illustrates the displacement of the phantom. The distance between the peak-to-peak displacement showed the consistency of movement for 3 mins (Fig.4b-c).

Table 1 shows the results of displacement according to the volume of the BVM. The volume of the BVM was manually controlled by the plastic plate selection, which was placed between the BVM and the linear actuator. Different thicknesses of the plate resulted in a different range of motion of the phantom. This allowed the tissue-mimicking phantom (1.2kg) to make a stable displacement of up to 9 mm.

4. Discussion

In this study, we have developed a low-cost, easy-to-make respiratory motion simulator to simulate respiration-induced abdominal organ motion. The proposed design did not require any software programming and can be easily assembled using 3D-printed components.

The design of the simulator was compatible with a clinical MRgFUS system with the ultrasound transducer built into the MRI table. The simulator assembly could be positioned over the transducer built into the MRgFUS table. The ring-shaped plastic holder with wheels could smoothly move the phantom without interrupting an ultrasound pathway from the table. All parts of the simulator could be easily 3D-printed and assembled following the instructions available in the open-source repository.

For the linear actuator, adequate torque power of the motor was needed to control the volume of the BVM as well as the volume of the Tygon tube and inflatable bag in the phantom. The DC motor in this study featured a torque of 6.8649 N·m and a speed of 16 rpm, which was enough to periodically deflate BVM. The motor speed controller allowed adjusting the respiratory rate in the range of 8-16 breaths/min. The motor and controller enabled to move the phantom weight of 1.2kg with various respiratory rates.

A fast MRI sequence integrated with a navigator tracking sequence was used for the evaluation of the designed simulator. Pixel size and signal-to-noise ratio of MR images could affect the accuracy of displacement measurements. Therefore, the motion analysis herein relied on navigator positions to avoid any uncertainty of the measurement. The measurement of navigator positions was consistent and stable during simulated inhalation and exhalation.

The main limitation of this study is that the simulator generated motion only in the superior/inferior direction. While SI is the major type of motion in abdominal organs, a realistic abdominal organ motion is much more complicated, including local deformation, a small movement in the lateral direction, cardiac motion, peristaltic movement, and any motion of the patient. In addition, the organ can move in any direction due to chest expansion and contraction. There are commercial respiratory simulators to support a programmable motion of the phantom in any direction, as well as speed control. This complex motion, however, may not be needed in many MRI pulse sequences and MR-guided therapy development projects.

Additionally, the range of displacement was limited by the volume of the BVM. The BVM used here allowed a maximum displacement of approximately 9 mm. This was sufficient for a proof-of-principle study for abdominal MRI acquisition techniques. Previous studies[22,23] reported the

averaged diaphragm motion amplitude of around 10.5 mm and the averaged displacement of pancreatic head and tail, kidneys, and spleen of 12.8, 13.0, and 14.3 mm, respectively. In future studies, a higher power motor and a higher elasticity of inflatable bag in the motion phantom will be investigated to achieve a wider range of displacement.

5. Conclusion

In this study, we presented a design for a low-cost MR-compatible respiratory motion simulator that can be easily replicated based on open-source 3D models and instructions. The simulator produced a periodic motion pattern, which simulated the motion of abdominal organs induced by respiration. We have demonstrated its ability to generate controlled respiratory motion of a phantom weighing 1.2 kg with the maximum displacement of approximately 9 mm. This could lower the barriers to the development of new MR imaging techniques with motion compensation.

Open Source

We have provided open-source files for the design, including the CAD files and supplement files. This source can be found as follows: https://github.com/mri-kisoo/RespiMotionSimulator

Acknowledgments

This study was funded by grants: NIH R21EB026018, R01EB025990, and R21CA230120.

Conflict of interest

The authors have no relevant conflicts of interest to declare.

Reference

1. Tokuda J, Morikawa S, Haque HA, Tsukamoto T, Matsumiya K, Liao H, Masamune K, Dohi T. Adaptive 4D MR Imaging Using Navigator-Based Respiratory Signal for MRI-Guided Therapy. Magnetic Resonance in Medicine. 2008;59(5):1051–1061. doi:10.1002/mrm.21436

2. Ferrer CJ, Bos C, Senneville BD de, Borman P, Stemkens B, Tijssen R, Moonen C, Bartels L. A planning strategy for combined motion-assisted/gated MR guided focused ultrasound treatment of the pancreas. International Journal of Hyperthermia. 2019;36(1):701–710. doi:10.1080/02656736.2019.1629650

3. Siedek F, Yeo SY, Heijman E, Grinstein O, Bratke G, Heneweer C, Puesken M, Persigehl T, Maintz D, Grüll H. Magnetic Resonance-Guided High-Intensity Focused Ultrasound (MR-HIFU): Technical Background and Overview of Current Clinical Applications (Part 1). RoFo: Fortschritte Auf Dem Gebiete Der Rontgenstrahlen Und Der Nuklearmedizin. 2019;191(6):522–530. doi:10.1055/a-0817-5645

4. Izadifar Z, Izadifar Z, Chapman D, Babyn P. An Introduction to High Intensity Focused Ultrasound: Systematic Review on Principles, Devices, and Clinical Applications. Journal of Clinical Medicine. 2020;9(2). doi:10.3390/jcm9020460

5. Chu W, Staruch RM, Pichardo S, Tillander M, Köhler MO, Huang Y, Ylihautala M, McGuffin M, Czarnota G, Hynynen K. Magnetic Resonance-Guided High-Intensity Focused Ultrasound Hyperthermia for Recurrent Rectal Cancer: MR Thermometry Evaluation and Preclinical Validation. International Journal of Radiation Oncology, Biology, Physics. 2016;95(4):1259–1267. doi:10.1016/j.ijrobp.2016.03.019

6. Zhu L, Lam D, Pacia CP, Gach HM, Partanen A, Talcott MR, Greco SC, Zoberi I, Hallahan DE, Chen H, et al. Characterization of magnetic resonance-guided high-intensity focused ultrasound (MRgHIFU)-induced large-volume hyperthermia in deep and superficial targets in a porcine model. International Journal of Hyperthermia. 2020;37(1):1159–1173. doi:10.1080/02656736.2020.1825836

7. Vigen KK, Daniel BL, Pauly JM, Butts K. Triggered, navigated, multi-baseline method for proton resonance frequency temperature mapping with respiratory motion. Magnetic Resonance in Medicine. 2003;50(5):1003–1010. doi:https://doi.org/10.1002/mrm.10608

8. Chen GT, Jiang SB, Kung J, Doppke KP, Willett CG. Abdominal organ motion and deformation: implications for IMRT. International Journal of Radiation Oncology, Biology, Physics. 2001;51(3):210. doi:10.1016/S0360-3016(01)02209-X

9. Bour P, Ozenne V, Marquet F, Senneville BD de, Dumont E, Quesson B. Real-time 3D ultrasound based motion tracking for the treatment of mobile organs with MR-guided high-intensity focused ultrasound. International Journal of Hyperthermia. 2018;34(8):1225–1235. doi:10.1080/02656736.2018.1433879

10. Celicanin Z, Auboiroux V, Bieri O, Petrusca L, Santini F, Viallon M, Scheffler K, Salomir R. Real-time method for motion-compensated MR thermometry and MRgHIFU treatment in abdominal organs. Magnetic Resonance in Medicine. 2014;72(4):1087–1095. doi:10.1002/mrm.25017

11. Hey S, Maclair G, Senneville BD de, Lepetit-Coiffe M, Berber Y, Köhler MO, Quesson B, Moonen CTW, Ries M. Online correction of respiratory-induced field disturbances for continuous MR-thermometry in the breast. Magnetic Resonance in Medicine. 2009;61(6):1494–1499. doi:10.1002/mrm.21954

12. Grissom WA, Rieke V, Holbrook AB, Medan Y, Lustig M, Santos J, McConnell MV, Pauly KB. Hybrid referenceless and multibaseline subtraction MR thermometry for monitoring thermal therapies in moving organs. Medical Physics. 2010;37(9):5014–5026. doi:10.1118/1.3475943

13. Han F, Zhou Z, Cao M, Yang Y, Sheng K, Hu P. Respiratory motion-resolved, self-gated 4D-MRI using rotating cartesian k-space (ROCK). Medical Physics. 2017;44(4):1359–1368. doi:10.1002/mp.12139

14. Cai J, Chang Z, Wang Z, Segars WP, Yin F-F. Four-dimensional magnetic resonance imaging (4D-MRI) using image-based respiratory surrogate: A feasibility study. Medical Physics. 2011;38(12):6384–6394. doi:10.1118/1.3658737

15. Liu X, Li C, Zhu J, Gong G, Sun H, Li X, Sun M, Zhang Z, Li B, Yin Y, et al. Technical Note: End-to-end verification of an MR-Linac using a dynamic motion phantom. Medical Physics. 2021;48(9):5479–5489. doi:10.1002/mp.15057

16. Fatemi-Ardekani A, Wronski M, Kim A, Stanisz G, Sarfehnia A, Keller B. SU-E-J-209: Geometric Distortion at 3T in a Commercial 4D MRI-Compatible Phantom. Medical Physics. 2015;42(6Part10):3313–3313. doi:10.1118/1.4924295

17. Maier-Hein L, Pianka F, Müller SA, Rietdorf U, Seitel A, Franz AM, Wolf I, Schmied BM, Meinzer H-P. Respiratory liver motion simulator for validating image-guided systems ex-vivo.

International Journal of Computer Assisted Radiology and Surgery. 2008;2(5):287–292. doi:10.1007/s11548-007-0140-2

18. Black DG, Yazdi YO, Wong J, Fedrigo R, Uribe C, Kadrmas DJ, Rahmim A, Klyuzhin IS. Design of an anthropomorphic PET phantom with elastic lungs and respiration modeling. Medical Physics. 2021;48(8):4205–4217. doi:10.1002/mp.14998

19. Kim K. Respiratory Motion Simulator. Thermal Therapy Research Group, University of California, San Francisco; 2021. https://github.com/mri-kisoo/RespiMotionSimulator

20. Santos JM, Wright GA, Pauly JM. Flexible real-time magnetic resonance imaging framework. The 26th Annual International Conference of the IEEE Engineering in Medicine and Biology Society;2004:1048–1051. doi:10.1109/IEMBS.2004.1403343

21. Holbrook AB, Santos JM, Kaye E, Rieke V, Pauly KB. Real-time MR thermometry for monitoring HIFU ablations of the liver. Magnetic Resonance in Medicine. 2010;63(2):365–373. doi:10.1002/mrm.22206

22. Liu C, Pierce LA, Alessio AM, Kinahan PE. The impact of respiratory motion on tumor quantification and delineation in static PET/CT imaging. Physics in Medicine and Biology. 2009;54(24):7345–7362. doi:10.1088/0031-9155/54/24/007

23. Kim YS, Park SH, Ahn SD, Lee JE, Choi EK, Lee S, Shin SS, Yoon SM, Kim JH. Differences in abdominal organ movement between supine and prone positions measured using four-dimensional computed tomography. Radiotherapy and Oncology: Journal of the European Society for Therapeutic Radiology and Oncology. 2007;85(3):424–428. doi:10.1016/j.radonc.2007.10.031

Figure Captions

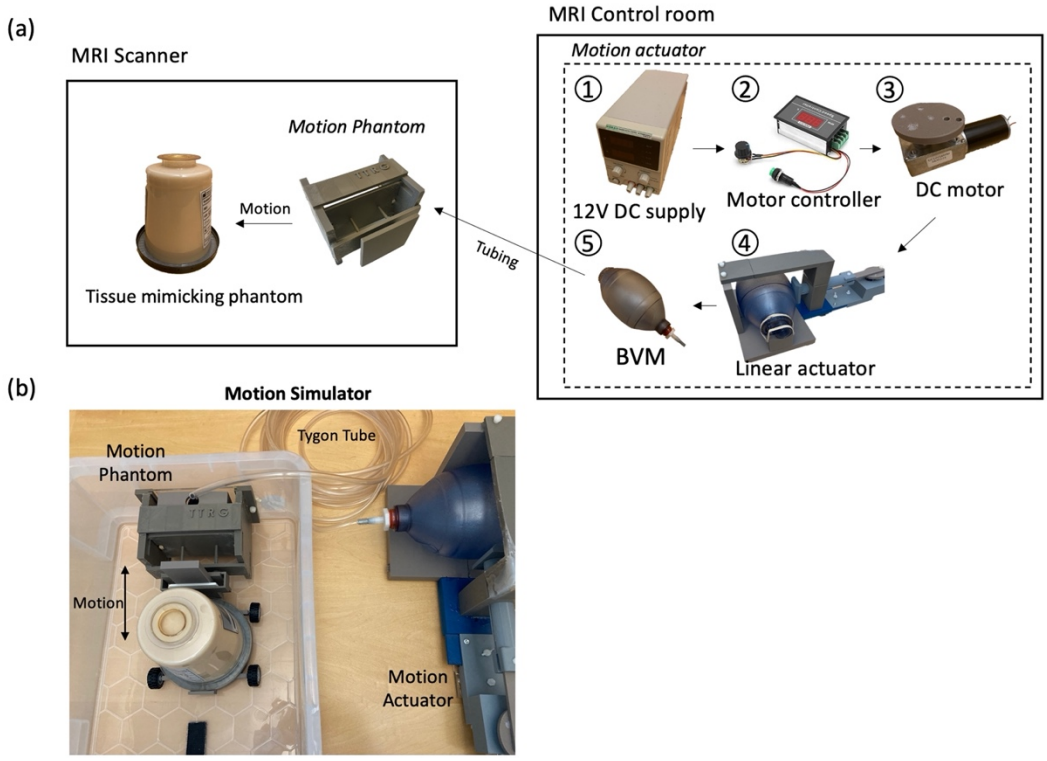

Figure 1. Design of the respiratory motion simulator. (a) A schematic diagram and (b) a photo of the phantom and actuator. Outside the MRI scanner, a DC motor and a controller are connected to a motion actuator, which increases or decreases the pressure inside the BVM. The BVM is coupled via the Tygon tube to the compressible bag in the motion phantom in the MRI scanner. Various levels of inflation or deflation of the BVM cause cyclical motion of tissue-mimicking phantom in the MRI scanner to simulate the shift of abdominal organs due to respiratory motion.

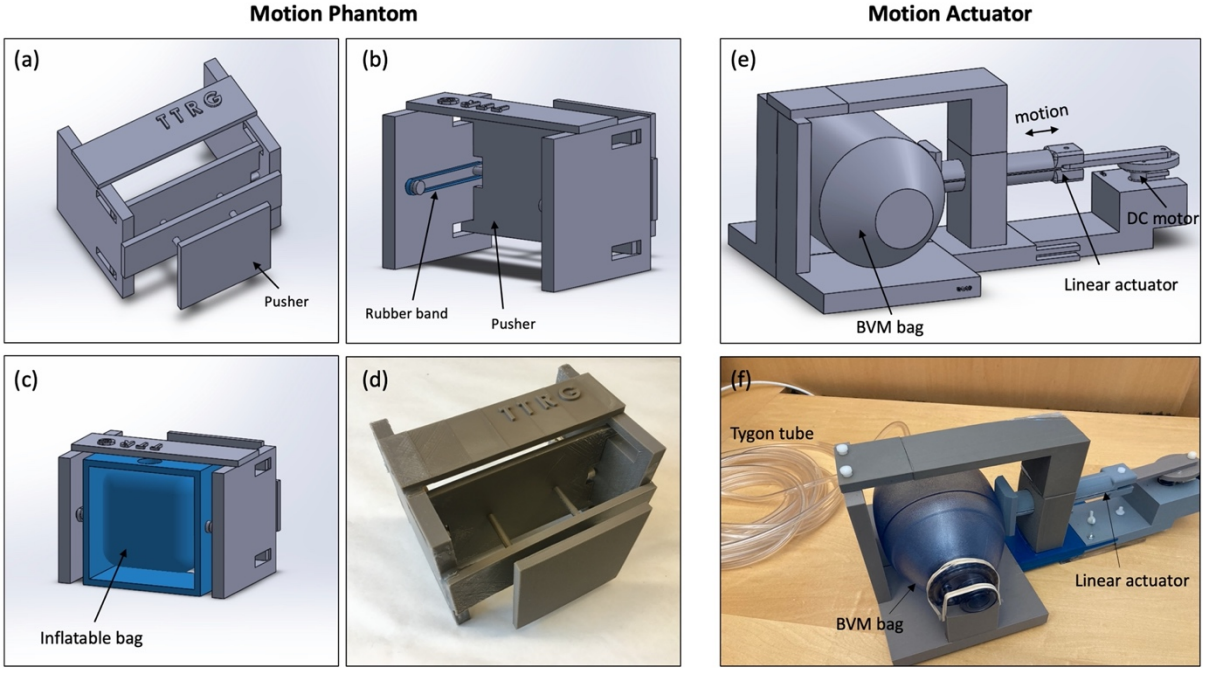

Figure 2. 3D models and photos for the motion phantom and actuator. (a-c) a 3D CAD model of the phantom viewing with different angles and (d) a photo of the 3D-printed phantom. (e) A 3D CAD model and (f) a photo of the motion actuator. An inflatable bag in the simulator is coupled with the BVM via the Tygon tube.

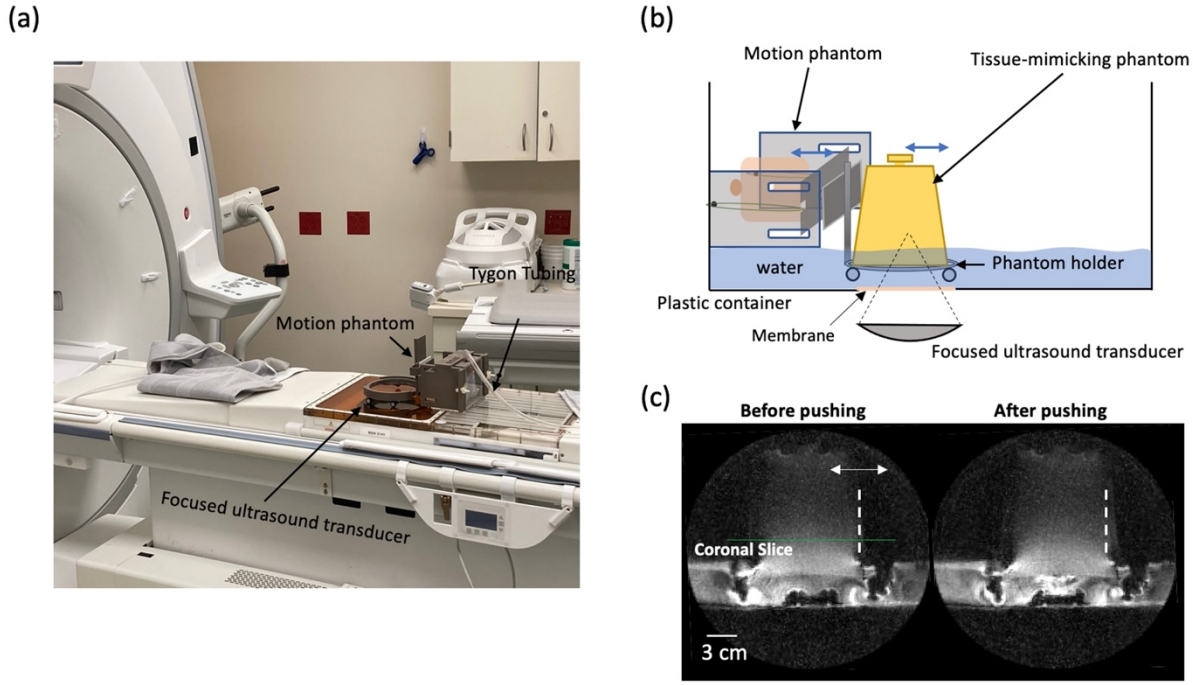

Figure 3. Photo (a) and illustration (b) of the motion phantom placement in the MRgFUS system. The phantom can be set in a plastic container (not shown in the photo) with a membrane on the bottom to allow acoustic propagation into the phantom. (c) MR sagittal magnitude images before/after pushing the phantom. Coronal slice was selected to evaluate the displacement of the phantom in this study.

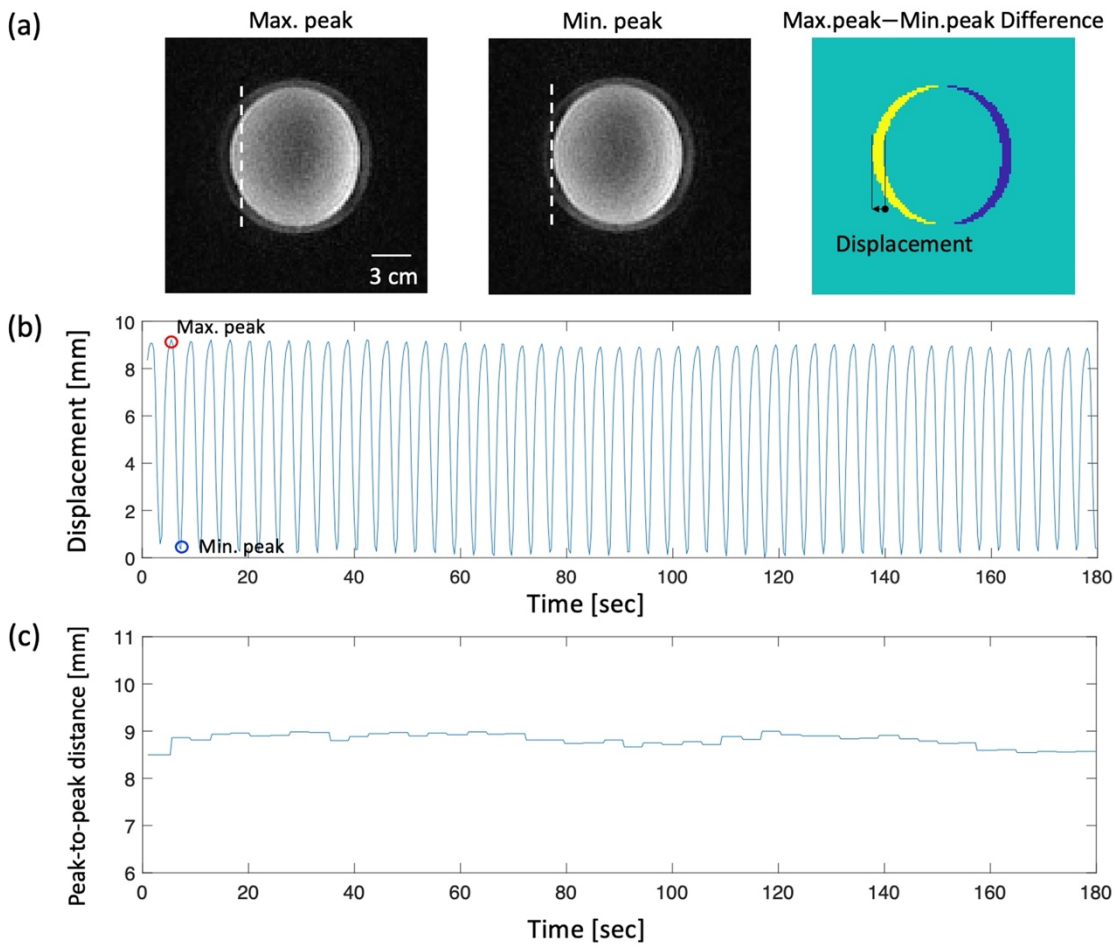

Figure 4. Measurement of the displacement of the phantom with 1.65 L volume of the BVM. MR magnitude images (a, left, center) were acquired on the coronal plane. White dashed lines indicate the original position of the phantom. (b) The displacement profile shows consistent and stable periodic motion for 3 minutes. Red and blue circles indicate the maximum and minimum peaks of the navigator position, respectively, that correspond to the magnitude images above. (c) Distance between the peak-to-peak displacement for 3 minutes is plotted to evaluate the consistency of movement.